JOURNAL OF THE ROYAL SOCIETY Interface

J. R. Soc. Interface (2006) **3**, 767–775
doi:10.1098/rsif.2006.0145
Published online 15 August 2006

Biological tolerance of different materials in bulk and nanoparticulate form in a rat model: sarcoma development by nanoparticles

Torsten Hansen[1,*], Gaëlle Clermont[2], Antonio Alves[2], Rosy Eloy[2], Christoph Brochhausen[1], Jean Pierre Boutrand[2], Antonietta M. Gatti[3] and C. James Kirkpatrick[1]

[1]*Institute of Pathology, Johannes Gutenberg-University of Mainz, Langenbeckstr. 1, 55101 Mainz, Germany*
[2]*Biomatech S.A., Zone Industrielle de I'Islon, 115 Rue Pasteur, 38670 Chasse-sur-Rhône, France*
[3]*Laboratorio dei Biomateriali, Universita degli studi di Modena e Reggio Emilia, Via Campi 231a, 41100 Modena, Italy*

In order to study the pathobiological impact of the nanometre-scale of materials, we evaluated the effects of five different materials as nanoparticulate biomaterials in comparison with bulk samples in contact with living tissues. Five groups out of 10 rats were implanted bilaterally for up to 12 months with materials of the same type, namely TiO_2, SiO_2, Ni, Co and polyvinyl chloride (PVC), subcutaneously with bulk material on one side of the vertebral column and intramuscularly with nanoparticulate material on the contralateral side. At the end of each implantation time, the site was macroscopically examined, followed by histological processing according to standard techniques. Malignant mesenchymal tumours (pleomorphic sarcomas) were obtained in five out of six cases of implanted Co nanoparticle sites, while a preneoplastic lesion was observed in an animal implanted with Co in bulk form. In the Ni group, all animals rapidly developed visible nodules at the implanted sites between 4 and 6 months, which were diagnosed as rhabdomyosarcomas. Since the ratio of surface area to volume did not show significant differences between the Ni/Co group and the TiO_2/SiO_2/PVC group, we suggested that the induction of neoplasia was not mediated by physical effects, but was mediated by the well-known carcinogenic impact of Ni and Co. The data from the Co group show that the physical properties (particulate versus bulk form) could have a significant influence on the acceleration of the neoplastic process.

Keywords: biomaterials; *in vivo* model; sarcoma; nanoparticles; cobalt; nickel

1. INTRODUCTION

Nanotechnology is a novel multidisciplinary branch of science, which has made a remarkable development in the last two decades. In numerous fields of medicine, nanoparticles hold great promises, for example, in imaging and drug delivery. Since nanoparticles have, by definition, a size of a few hundred nanometres at maximum, they have the possibility of interfering with several subcellular mechanisms. Thus, they are being discussed as possible vehicles in gene therapy on the one hand (Kirchweger 2002), and on the other hand, there are reservations about possible cytotoxicity, inflammatory response and malignant transformation. In this context, one of the most important aspects is the release of particulate matter by wear and corrosion of conventional implants (Revell *et al.* 1997; Peters *et al.* 2004). These different pathobiological reactions are essential elements in the characterization of the biological tolerance of different particulate materials.

In a recent study, our group examined the biological tolerance of different nano-scaled particles, i.e. PVC, TiO_2, SiO_2, Co and Ni, following interaction with endothelial cells *in vitro*, which are ubiquitous in the living organism (Peters *et al.* 2004). Although most particle types were internalized (except Ni particles), only Co particles possessed cytotoxic effects. In order to examine the biological tolerance of the above-mentioned particles *in vivo*, we used a rodent implantation model to evaluate the effect of these five different materials under two modes of application (bulk samples and nanoparticles) in direct contact for 6–12 months

*Author for correspondence (hansen@pathologie.klinik.uni-mainz.de).

Received 13 June 2006
Accepted 7 July 2006

Table 1. Test materials. (B, Bulk material; NP, nanoparticulate material; Ø, diameter (mm); *H*, height (mm).)

nanoparticles	TiO_2		SiO_2		Ni		Co		PVC	
form	B	NP	B	NP	B	NP	B	NP	B	NP
material number	1	2	3	4	5	6	7	8	9	10
presentation	Ø : 0.9, *H* : 1	20–30 mg	Ø : 12, *H* : 1	3–7 mg	Ø : 10, *H* : 1	10–125 mg	Ø : 6.5, *H* : 1	60–100 mg	Ø : 10, *H* : 1	50–60 mg
ratio of surface area to volume (mm^{-1})	3.9	9×10^4	3.85	4×10^5	4.13	600	4.73	5×10^4	4.2	5×10^4
quantity of samples used	10	10	10	10	10	10	10	10	10	10
storage conditions	room temperature									

with the subcutaneous or muscular tissues, respectively. Besides clinical and macroscopic examination, tissue specimens were analysed by conventional light microscopy and immunohistochemistry.

2. MATERIAL AND METHODS

Five different materials, i.e. titanium dioxide (TiO_2), silicon dioxide (SiO_2), nickel (Ni), cobalt (Co) and polyvinyl chloride (PVC), were considered under two forms, namely bulk and nanoparticulate state, as summarized in table 1. They were selected on the basis of their chemical and physical properties, especially in relation to their biocompatibility. Ni and Co are metals that can corrode with the release of metallic ions, whereas TiO_2 and SiO_2 are ceramic materials, which are chemically inert. Finally, PVC is a polymer without any additive such as phthalates.

TiO_2 and SiO_2 particles were produced by flame spray pyrolysis (TAL Materials, Inc., Ann Arbor, MI, USA). The size spectrum of SiO_2 particles was between 4 and 40 nm with a mean particle size of 14 nm. The size of TiO_2 particles was between 20 and 160 nm with a mean particle size of 70 nm. The size of Co particles (Sigma Chemicals, Deisenhofen, Germany) was between 50 and 200 nm (average size 120 nm). Ni particles were made by closed circuit pulverization (University of Bologna, Italy). Their mean crystallite size was 50 nm. The PVC particles possessed a mean particle size of 130 nm with a size distribution between 60 and 170 nm (European Vinyl Corporation International, Cheshire, UK). The ratio of surface area to volume is listed in table 1. Among the bulk material forms, Co showed the highest value ($4.73\ mm^{-1}$) and SiO_2 the lowest value ($3.85\ mm^{-1}$), while among the nanoparticles, SiO_2 revealed the highest value ($4\times10^5\ mm^{-1}$) and Ni the lowest value ($600\ mm^{-1}$). It should be mentioned that the latter value was owing to an agglomeration of particles with a mean size of 10 μm after the intramuscular injection. These agglomerates could be found in intramuscular localization by radiography of the respective tissue specimens (data not shown). Using the original diameter of 50 nm, a value of $1.2\times10^5\ mm^{-1}$ can be obtained.

Five groups out of 10 Sprague–Dawley rats (all male; IFFA Credo, France) were implanted for 6, 8 or 12 months (see table 2). In each group, 10 animals were implanted bilaterally with the same material, i.e. subcutaneously with bulk material, and intramuscularly with nanoparticulate material for each animal. While it would have been desirable to have the same type of implantation site for each material form, the bulk material was used subcutaneously, as this is the most frequently used site in other studies. The nanoparticulate material had to be implanted intramuscularly in order to restrict it to an enclosed focus, which would enable the peri-implant area for histology to be precisely defined. The dimensions of the bulk material are given in table 1. Animals were anaesthetized by intramuscular injection of tiletamine–zolazepam ($50\ mg\ kg^{-1}$). An incision large enough to accommodate the sample was made on one side of the back through the skin and parallel to the vertebral

Table 2. Study design and macroscopic observations. (The material numbers refer to those in table 1.)

material	1	2	3	4	5	6	7	8	9	10	total
number of animals	10		10		10		10		10		
subcutaneous (s.c.) sites	10	—	10	—	10	—	10	—	10	—	50
intramuscular (i.m.) sites	—	10	—	10	—	10	—	10	—	10	50
visible nodule development (sites)	0	0	0	0	10	10	0	10	0	0	30
sacrifice or death (animals)											
4–5 months		0		0		3[a]		0		0	3
6 months		4		4		7[b]		4		4	23
8 months		0		0		0		1[a]+5[b]		0	6
12 months		6		6		0		0		6	18

[a] Death of the animal.
[b] Animals were euthanized because of the development of handicapping tumours.

column. A pocket was formed by blunt dissection in the subcutaneous tissue in which the implant material was introduced. The bulk material was implanted on the right side of the vertebral column of each animal. On the left side of each animal, implantation of nanoparticulate material (same nanoparticulate type as for the bulk material) was performed in the paravertebral muscle, the particles covering an area of approximately 2 cm^2. The skin was closed with metallic staples. The rats were returned to their respective cages and observed for recovery from the anaesthetic.

The husbandry of the animals was in keeping with the European standard requirements. Complete rat maintenance diet was given in pellet form in addition to water *ad libitum*. Animals were observed daily for any clinical abnormality.

At the end of the observation period, each animal was euthanized by injection of sodium pentobarbital-based drug. Complete autopsy of each animal was performed in addition to careful study of the regions of interest in the subcutaneous and intramuscular tissue (implantation sites). Local macroscopical features such as necrosis, exudates, haemorrhage, fibrous tissue, etc. were documented and the tissue was conserved for histopathological examination.

Each site was fixed in 4% phosphate-buffered saline (PBS)-buffered formalin, processed according to standard protocols and embedded in paraffin. Sections of 4–5 μm thickness were cut and stained by safrin–haematoxylin. To detect the PVC particles, Oil Red reaction was additionally performed, since this has been described as a useful staining for polymeric particles like polyethylene (Hansen *et al.* 2002). In several cases, the Giemsa stain was also applied. In addition, tissue specimens of the Co and Ni groups were examined by immunohistochemistry using the avidin–biotin–peroxidase complex method. The antibodies (markers shown in table 3) were first applied according to the manufacturer's recommendations on non-tumourous rat tissue in order to delineate the optimal pretreatment and dilution for the implanted tissue specimens.

Slides were examined and photographed using a Leica microscope (Dialux, Leica Microsystems, Wetzlar, Germany; Nikon camera, Nikon, Germany).

3. RESULTS

A summary of macroscopic and microscopic findings is presented in tables 2 and 4.

3.1. TiO_2

In all cases, a thin fibrous capsule surrounding the bulk material implanted subcutaneously was observed, without any significant macroscopic sign of local intolerance. The bulk material did not reveal any abnormality. Histologically, the tissue specimens of implanted bulk materials exhibited moderate inflammatory infiltrates, but no granulomas. Moreover, moderate fibrosis was found, which was accompanied by discrete capillarization in the periphery of the fibrotic area.

Table 3. Primary antibodies.

marker	specificity	manufacturer	pre-treatment	dilution
S100	rabbit anti-bovine[a]	Dako (Denmark)	0.1% trypsin	1 : 2500
desmin	mouse anti-human[a]	Dako	3×5 min microwave (600 W)	1 : 100
myogenin	mouse anti-rat	Dako	3×5 min microwave (600 W)	1 : 25
PCNA	mouse anti-rat	Dako	3×5 min microwave (600 W)	ready to use

[a] Cross-reactivity with rat tissue confirmed by the manufacturer.

Table 4. Synopsis of the histological findings. (B, Bulk material; NP, nanoparticulate material.)

material	6-month period	12-month period
TiO : NP	granuloma	granuloma
TiO : B	inflammation	inflammation
SiO : NP	inflammation	inflammation
SiO : B	inflammation	inflammation
PVC : NP	granuloma	granuloma + fibroblastic proliferation
PVC : B	inflammation	inflammation
Co : NP	preneoplasia	neoplasia[a]
Co : B	inflammation + granuloma	preneoplasia[a]
Ni : NP	neoplasia	[b]
Ni : B	neoplasia	[b]

[a] Animals were euthanized after eight months.
[b] No analysis—animals were euthanized after six months.

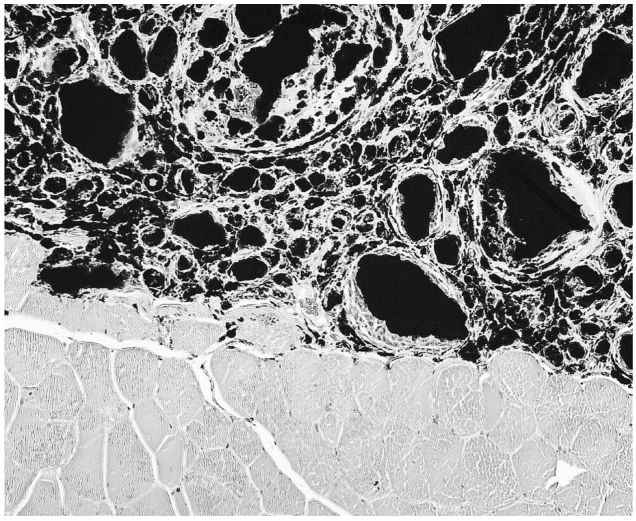

Figure 1. Implanted TiO_2 nanoparticles reveal aggregates which were surrounded by macrophages and multinucleated giant cells forming granuloma (haematoxylin and eosin (HE) stain, objective magnification ×20).

The sites implanted with nanoparticles revealed the presence of a whitish paste at the site of implantation in the intramuscular tissue without any local evidence of intolerance. Histological examination of all implanted particle sites revealed prominent intramuscular foreign body granulomas. Macrophages and foreign body giant cells surrounded abundant extracellular black granules, which did not reveal birefringence in polarized light (figure 1). In few cases, moderate fibrosis in and around the granulomas could be found.

3.2. SiO_2

In all cases, an adherent thin fibrous capsule surrounding the bulk material implanted subcutaneously was observed, without any significant macroscopic evidence of local intolerance. Histological analysis of the implanted bulk material revealed a fibrotic capsule and an inflammatory infiltrate consisting mainly of lymphocytes and monocytes, with no increase of mast cells.

At the site of intramuscular implantation, no particles were visible and no macroscopic abnormality was observed. Histological examination of the specimens with implanted particles revealed chronic inflammatory infiltrates, which were localized subcutaneously and intramuscularly. Besides the inflammatory infiltrates, increased numbers of mast cells (up to 10 mast cells per high-power field (HPF)) could be found in most cases. These cells were typically localized perivascularly (figure 2).

3.3. PVC

In all cases, a thin fibrous pocket surrounding the bulk material implanted subcutaneously was observed, without any local macroscopic lesion. The bulk material itself did not reveal any abnormality. Histological evaluation of implanted PVC bulk showed discrete chronic inflammatory infiltrates intermingled with few mast cells. No particles were observed.

The sites with implanted nanoparticles were also macroscopically unremarkable. In 8 out of 10 animals, particulate matter was macroscopically visible in the subcutaneous tissue. On histology, all cases of implanted PVC nanoparticles revealed intramuscular foreign body-type granuloma. Macrophages and multinucleated foreign body giant cells were seen surrounding amorphous, unstained polygonal material that did not exhibit birefringency under polarized light (figure 3). However, the particles revealed intense cherry red colour by staining with the Oil Red reaction (figure 4). A slight peri-granulomatous fibrosis was also seen. Most interestingly, we observed the foci of fibroblastic proliferation in three animals. The cells were spindle-shaped and showed some nuclear pleomorphism. On immunohistochemistry, they revealed an enhanced nuclear expression of the proliferation marker, proliferating cell nuclear antigen (PCNA).

3.4. Co

Clinical examination revealed the occurrence of subcutaneous and intramuscular nodules, which appeared at the nanoparticle implanted sites in three animals of the

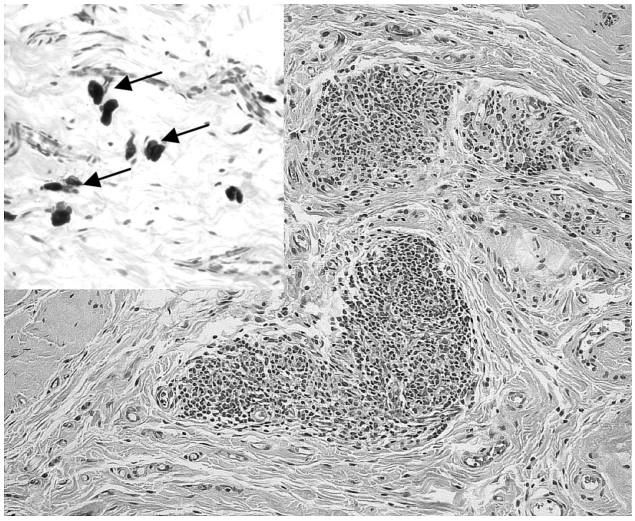

Figure 2. Tissue specimen from an animal of the SiO_2 group reveals inflammatory infiltrates at the site implanted with nanoparticulate material. Inset demonstrates several mast cells (arrows; HE stain, objective magnification ×20, inset ×40).

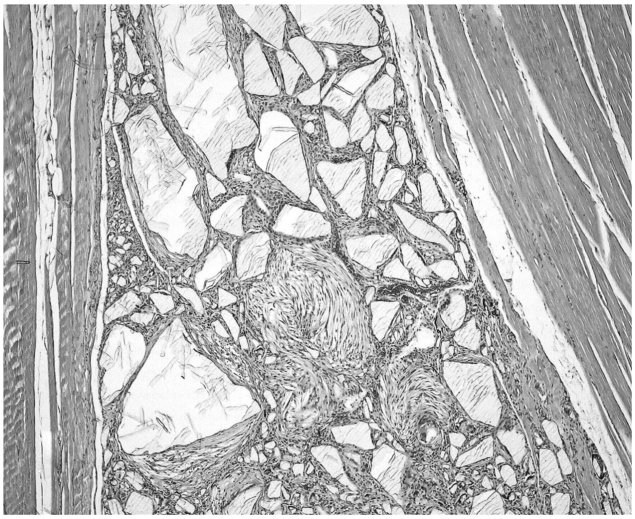

Figure 3. Implanted PVC nanoparticles show aggregates surrounded by granulomas (HE stain, objective magnification ×10).

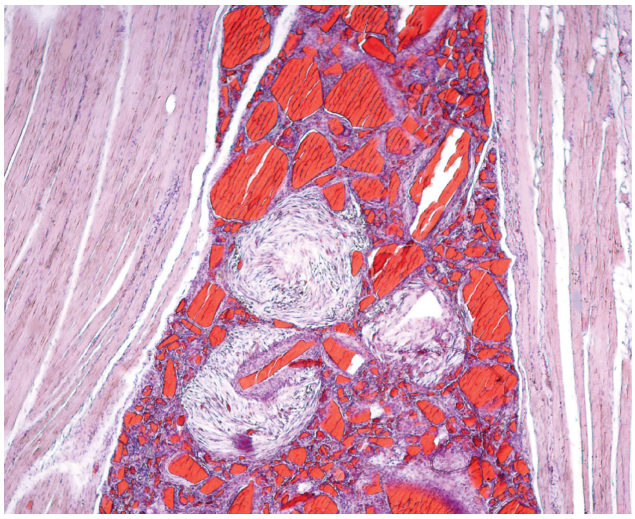

Figure 4. Same animal as in figure 3 displays Oil Red-positive particles (Oil Red stain, objective magnification ×10).

Figure 5. Animal implanted with Co nanoparticles on the left side exhibiting clearly visible nodule.

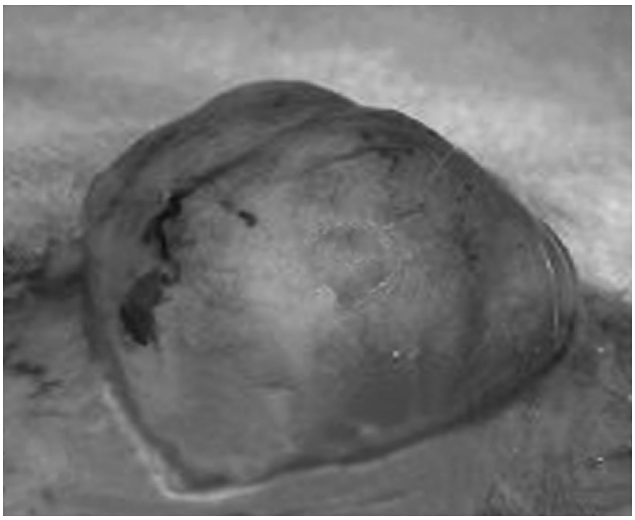

Figure 6. Nodule from figure 5 shows an encapsulated and vascularized tumour mass.

Co group after six months. Subsequently, all the remaining animals implanted with Co developed nodules at the sites of implanted nanoparticles (figures 5 and 6). One animal of the 12-month observation group died eight months following implantation and for ethical reasons, all the remaining animals were sacrificed at eight months, owing to the development of these handicapping tumours. In three of the four cases of the six-month observation period and in all six cases of the eight-month observation period, nodules developed at the nanoparticle-implanted site. In almost all the cases, a thin translucent non-adherent capsule around the bulk material implanted subcutaneously was observed.

Histological examination of the specimens with implanted nanoparticles demonstrated malignant mesenchymal tumours in one of the four animals from the six-month observation period and in five out of six cases from the eight-month observation period. The tumour was localized intramuscularly, i.e. at the original implantation site. The tumour cells were typically spindle-shaped and showed a high degree of

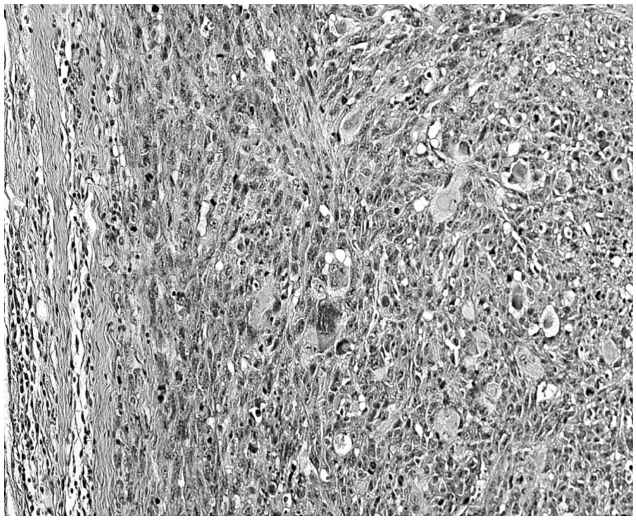

Figure 7. Malignant mesenchymal tumour of an animal with implanted Co particles. Numerous multinucleated tumour giant cells are noted (HE stain, objective magnification ×20).

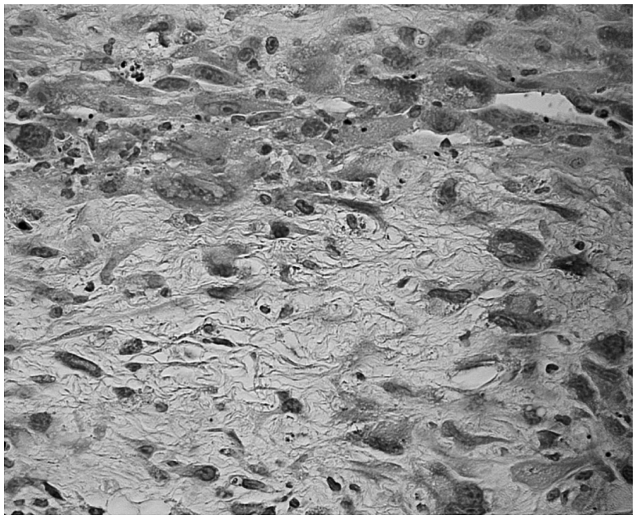

Figure 8. Tissue around Co bulk displays mesenchymal cells with enhanced nuclear cytoplasmic ratio as well as pleomorphism and prominent nucleoli (HE stain, objective magnification ×40).

atypia with atypical mitoses. Besides multinucleated histiocytic giant cells, bizarre tumour giant cells were observed (figure 7). Central necrosis was partially prominent. Immunohistochemically, the tumour cells were negative for S-100 and myogenin and only focally positive for desmin, suggesting that they resembled undifferentiated high-grade pleomorphic sarcomas (hence called sarcomas, unless otherwise specified). Particles were observed in three out of six animals in the eight-month observation period.

In two out of four animals of the six-month observation period (at the nanoparticulate site) and in two further animals of the eight-month observation period (one at the nanoparticles' site and one around bulk material), we found a capsule with fibroblastic proliferations. The cells revealed increased pleomorphism of the nuclei and mitotic rate (figure 8). In addition, they displayed strong expression of the proliferation marker, PCNA (figure 9). These lesions are classified as

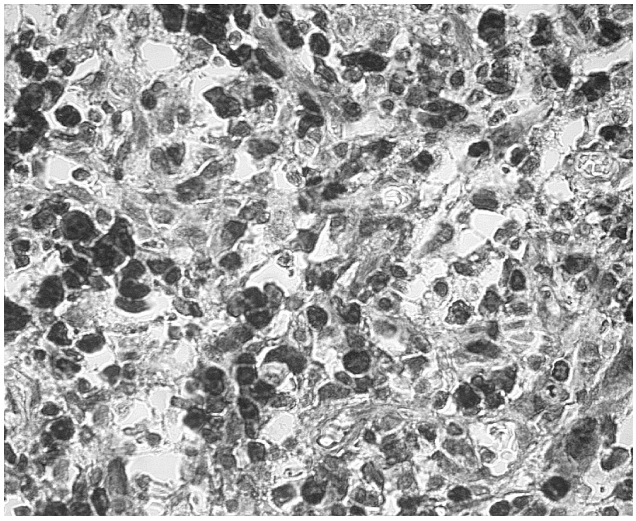

Figure 9. PCNA labelling of the same animal as in figure 8 reveals numerous positive nuclei (black) of the mesenchymal cells (diaminobenzidine tetrahydrochloride (DAB) stain, objective magnification ×40).

preneoplasia according to previous studies (Kirkpatrick *et al.* 2000).

Together, these results show a malignant mesenchymal tumour in five out of six cases of implanted Co nanoparticle sites and four other cases (one around bulk material and three at the nanoparticulate site) with preneoplasia.

By contrast, malignant mesenchymal tumours were not observed around the bulk material. Commonly, there was a discrete inflammatory infiltrate, composed of mononuclear cells and lymphocytes. In the subcutaneous area, a discrete fibrosis was observed, but granulomas were not found.

3.5. Ni

Three animals from the Ni-implanted group died 4, 4.5 and 5.5 months after implantation. On the basis of this mortality rate in this group and the development of tumours, it was decided to sacrifice all the remaining animals from the Ni-implanted group at six months. Both subcutaneous and intramuscular implantation sites developed visible nodules in all cases. In all cases, necrosis was observed inside the nodule associated with deposits and exudate seen in the implanted subcutaneous pocket.

Both forms of implanted Ni (i.e. bulk and nanoparticles) exhibited a malignant mesenchymal tumour, which was localized subcutaneously and intramuscularly. In general, the tumour was surrounded by a fibrous capsule. Tumour cells were spindle-shaped or showed a rhabdoid pattern (figures 10 and 11). Furthermore, multinucleated giant cells could be observed. These appeared to be of either neoplastic origin or myogenic origin (the so-called myogenic giant cells); some of them also resembled osteoclast-like giant cells. Cells revealed atypia and increased mitotic rate (up to seven mitoses per HPF). Furthermore, areas of central necrosis could be demonstrated. Immunohistochemistry showed strong cytoplasmic expression of

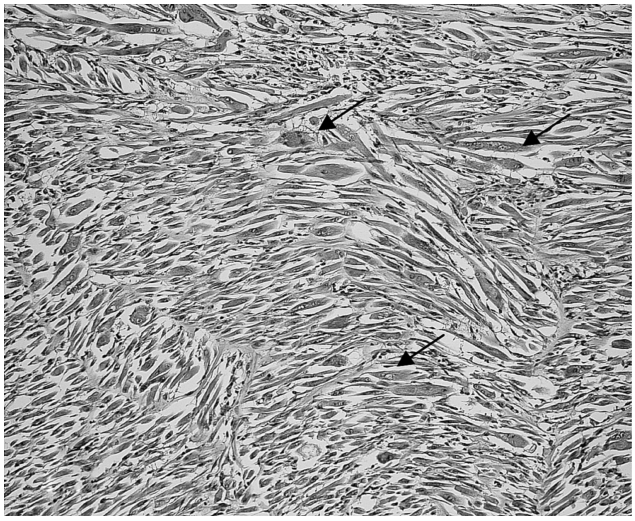

Figure 10. Animal from the Ni group with a malignant mesenchymal tumour exhibiting numerous multinucleated rhabdoid cells (arrows) with eccentric nuclei and prominent nucleoli (HE stain, objective magnification ×10).

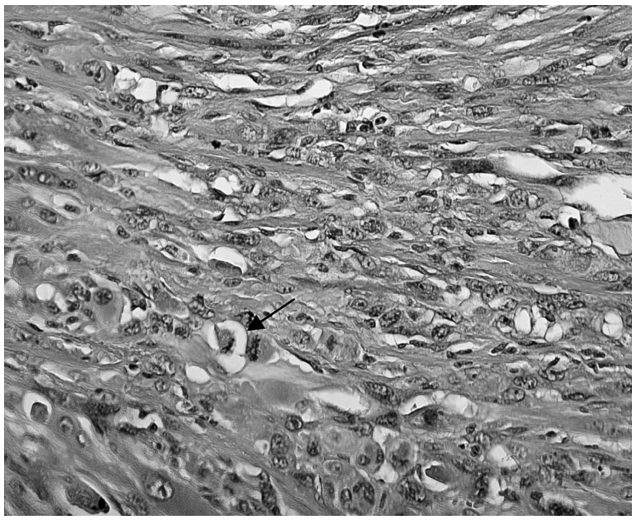

Figure 11. Detailed photograph of tumour of the Ni group shows prominent nuclear pleomorphism and some mitoses (arrow; HE stain, objective magnification ×20).

desmin and strong nuclear staining of myogenin in all the tumours examined (figure 12). In contrast, tumour cells were completely negative for S-100.

In the case of implanted nanoparticles, a prominent pleomorphism of the nuclei was common. In general, abundant areas of central necrosis, dystrophic calcification and ossification were also observed. In contrast, in tissue specimens implanted with bulk material, tumours showed a central cystic component, suggestive of the implant site. Furthermore, necrosis was less prominent, and ossification was only rarely seen. Particles could not be observed by means of histology. However, radiological examination of the paraffin blocks revealed dense material in several cases (data not shown). Moreover, in all the specimens, there were many haemosiderin-laden cells, suggestive of residual haemorrhage. Throughout all specimens, a faint to moderate lymphocytic inflammatory infiltrate was

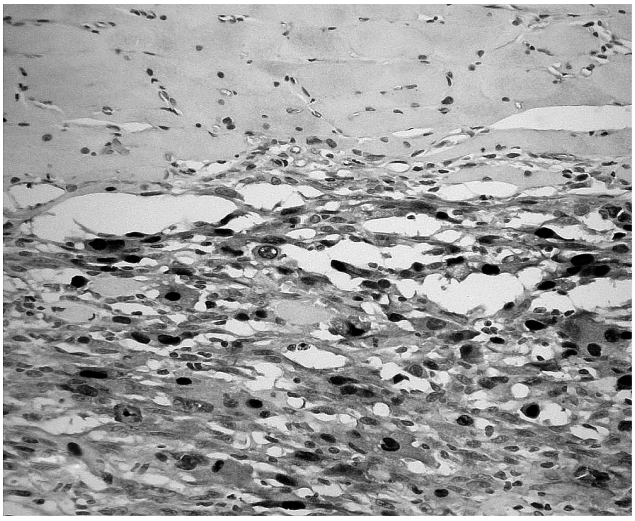

Figure 12. Immunohistochemistry of the same tissue as in figure 11 obtains numerous cells expressing myogenin (black) in the tumour (lower part) as well as the regional skeletal muscle (upper part; DAB stain, objective magnification ×20).

seen. Apart from the tumour giant cells (reported previously), no granulomas occurred.

Together, the findings indicate a malignant mesenchymal tumour, which is classified on the basis of the morphology and the immunohistochemical marker profile as rhabdomyosarcoma (Fletcher *et al.* 2002).

4. DISCUSSION

The objective of the present study was to evaluate the effect of five different materials under two modes of application (bulk samples and nanoparticles) in direct contact with the subcutaneous and muscular tissues for 6 or 12 months. This study design enabled the reaction at the tissue–material interface to be compared with respect to the physical form of the materials used. Concerning the toxicity and carcinogenic effect of different materials, several *in vitro* and *in vivo* studies have been performed with particles size in the range of micrometres (for review see Schins 2002). By contrast, this is the first *in vivo* study to our knowledge that examines the effects of particulate material in the nanometre range. The data of our investigation are summarized in table 4. Interestingly, tumours were observed only in Co- and Ni-implanted sites, but not in the remaining three materials.

The most variable lesions and also the most surprising observations were found in the Co group. In the animals implanted with bulk material, inflammation was observed after six months and preneoplasia after eight months. However, in the nanoparticle-implanted animals, we found preneoplasia and one case of malignant tumour after six months and malignant tumours (pleomorphic sarcomas) in almost all the cases after eight months. The carcinogenicity of cobalt and its compounds has been intensively investigated in the past decades (Shabaan *et al.* 1977; Ward *et al.* 1990; Lison *et al.* 2001). The carcinogenic potential of cobalt and its compounds was evaluated by the International Agency for Research on Cancer in 1991. It was concluded that there was

inadequate evidence of carcinogenicity in humans (lung cancer), but sufficient evidence in experimental animals. Thus, cobalt and its compounds were classified (Lison *et al.* 2001) as possibly carcinogenic in humans (group 2B). Since then, several studies have been undertaken, which demonstrated that the species of cobalt have different influences on the toxicity and carcinogenicity. As stated for the Ni data, it remains to be elucidated whether the present findings of the Co group can be extrapolated to possible effects in humans. Nevertheless, the findings of the Co group can be summarized for a model of neoplasia sequence as follows:

$$(\text{inflammation}\rightarrow)\ \text{preneoplasia} \rightarrow \text{neoplasia},$$

and thus follow the general concept of pathogenesis for malignant tumours, which has been proposed not only for carcinomas, but also for sarcomas (Kirkpatrick *et al.* 2000; Mentzel 2000; Lison *et al.* 2001). We therefore suggest that this model is suitable for the investigation of the detailed mechanisms of this sequence and can give novel insights in the pathogenesis of mesenchymal neoplasia. However, most significantly, the physical form of the cobalt, i.e. whether bulk or nanoparticulate, seems to play a central role in an acceleration of the neoplastic process.

With regard to the physical properties, both the surface area and the volume of the particles have been suggested to be critically involved in the cytopathological mechanisms (for review, see Oberdörster *et al.* 2005). However, in the present study the ratio of the surface area to volume did not show any difference between Ni and Co on the one hand and PVC, TiO_2 and SiO_2 on the other hand for both the particles group and the bulk group (see table 1). Moreover, in the Ni group, malignant mesenchymal tumours were found both in the nanoparticles and the bulk implanted animals. This favours the view that, particularly in the case of Ni and Co, well-known chemical effects of these elements (such as the alteration of cell-signalling pathways and the induction of DNA damage) play a vital role in the induction of neoplasia. From the results of the Co group, it can be deduced that the physical properties could have an influence on the acceleration of the neoplastic process.

One of the most impressive findings was the occurrence of malignant mesenchymal tumours in *all* animals of the Ni group. Tumours were found in sites implanted with both the bulk and the nanoparticles. According to the histomorphological and immunohistochemical findings, all these neoplasms could be classified as rhabdomyosarcomas. The carcinogenic effect of Ni has been intensely investigated in the last decades (for review, see Kasprzak *et al.* 2003). It is well established that human exposure to highly nickel-polluted environments can lead to cancer of the respiratory tract. Among these tumours, squamous cell carcinomas and anaplastic or undifferentiated carcinomas are mainly described. On the other hand, a number of studies have documented that the intramuscular induction of nickel compounds resulted in the development of rhabdomyosarcomas in rats (Damjanov *et al.* 1978; Sano *et al.* 1988; Nanni *et al.* 1991), while fibrosarcoma was predominantly observed in mice (Rodriguez *et al.* 1996). Most interestingly, Damjanov *et al.* (1978) also found rhabdomyosarcomas among the testicular neoplasms, which occurred after the injection of Ni_3S_2. The authors suggested that a malignant transformation of undifferentiated pluripotent mesenchymal cells was induced. This view could give an explanation for the observation of subcutaneous rhabdomyosarcomas at the site of bulk implantation as found in our study.

In contrast to the numerous reports of Ni-induced rhabdomyosarcomas in several animal studies, only very few data exist concerning the association between Ni exposure and rhabdomyosarcomas in humans (for review, see Kasprzak *et al.* 2003). The statistical significance of the increased risk of soft-tissue sarcomas after Ni exposition is doubtful (Kasprzak *et al.* 2003). Moreover, by using the same study design as presented in this study, we could not find any malignant transformation after implantation of five different materials in sheep, neither for Ni nor for the other materials (data not shown). In addition, it has been reported that in several rat strains, including the Sprague–Dawley rats (used in the present study), numerous malignant tumours can occur spontaneously (Kaspareit & Rittinghausen 1999; Nakazawa *et al.* 2001). In the study of Kaspareit & Rittinghausen (1999), mammary gland tumours were mainly observed. However, rhabdomyosarcoma was also found in one case. Further case reports of spontaneous rhabdomyosarcomas in Sprague–Dawley rats exist (Glaister 1981; Conner 1994). Together, the Ni-associated malignancy of the present study should be critically regarded concerning a deduction of possible effects in the human. Nevertheless, the rat implantation model described here presents an excellent tool to generate rhabdomyosarcomas, so that this system could be useful to research groups studying the molecular pathogenesis of rhabdomyosarcomas.

In summary, these data indicate that in the present animal model, the pathological processes observed are not simply owing to the physical properties of the particles, as demonstrated in the Co group. The chemical properties, most probably, play an additional role in the pathomechanisms underlying our postulated particle-dependent preneoplasia–neoplasia model. In this context, more detailed studies regarding the physical and chemical particle–tissue interactions are of vital interest for our understanding of nanobiology regarding the application of nanoparticles in medicine. Furthermore, it should be stressed that the rat implantation model for material-induced neoplasia cannot be extrapolated to the human *in vivo* situation. There is still no relevant animal model, which is able to predict possible biomaterial-induced neoplasia in humans.

This work was supported by the European Commission (QOL-2002-147). The authors wish to thank Vincent Boiza and Nadine Girod (Biomatech, France) as well as Silke Mitschke, Irmtrud Roth and Katharina Tokarska (Institute of Pathology, Mainz, Germany) for their excellent technical assistance. Finally, authors especially thank Herbert Radner (Institute of Pathology, Mainz, Germany) for careful co-examination of the tissue specimens.

REFERENCES

Conner, M. W. 1994 Spontaneous rhabdomyosarcoma in a young Sprague–Dawley rat. *Vet. Pathol.* **31**, 252–254.

Damjanov, I., Sunderman, F. W., Mitchell, J. M. & Allpass, P. R. 1978 Induction of testicular sarcomas in Fischer rats by intratesticular injection of Nickel subsulfide. *Cancer Res.* **38**, 268–276.

Fletcher, C. D. M., Unni, K. K. & Mertens, F. 2002 *Pathology and genetics of tumours of soft tissue and bone*. Lyon: IARC Press.

Glaister, J. R. 1981 Rhabdomyosarcoma in a young rat. *Lab. Anim.* **15**, 145–146.

Hansen, T. *et al.* 2002 New aspects in the histological examination of polyethylene wear particles in aseptically loosened total joint arthroplasties. *Acta histochem.* **104**, 263–269. (doi:10.1078/0065-1281-00649)

Kaspareit, J. & Rittinghausen, S. 1999 Spontaneous lesions in Harlan Sprague–Dawley rats. *Exp. Toxic. Pathol.* **51**, 105–107.

Kasprzak, K. S., Sunderman, F. W. & Salnikow, K. 2003 Nickel carcinogenesis. *Mutat. Res.* **533**, 67–97.

Kirchweger, G. 2002 Nanoparticles—The next big thing? *Mol. Ther.* **6**, 301–302. (doi:10.1006/mthe.2002.0686)

Kirkpatrick, C. J., Alves, A., Köhler, H., Kriegsmann, J., Bittinger, F., Otto, M., Williams, D. F. & Eloy, R. 2000 Biomaterial-induced sarcoma. A novel model to study preneoplastic change. *Am. J. Pathol.* **156**, 1455–1467.

Lison, D., De Boeck, M., Verougstraete, V. & Kirsch-Volders, M. 2001 Update on the genotoxicity and carcinogenicity of cobalt compounds. *Occup. Environ. Med.* **58**, 619–625. (doi:10.1136/oem.58.10.619)

Mentzel, T. 2000 Biological continuum of benign, atypical, and malignant mesenchymal neoplasms—does it exist? *J. Pathol.* **190**, 523–525. (doi:10.1002/(SICI)1096-9896(200004)190:5<523::AID-PATH578>3.0.CO;2-3#)

Nakazawa, M. *et al.* 2001 Spontaneous neoplastic lesions in aged Sprague–Dawley rats. *Exp. Anim.* **50**, 99–103. (doi:10.1538/expanim.50.99)

Nanni, P. *et al.* 1991 *In vitro* differentiation of rhabdomyosarcomas induced by nickel or by Moloney murine sarcoma virus. *Br. J. Cancer* **63**, 736–742.

Oberdörster, G., Oberdörster, E. & Oberdörster, J. 2005 Nanotoxicology: an emerging discipline evolving from studies of ultrafine particles. *Environ. Health Perspect.* **113**, 823–839.

Peters, K., Unger, R. E., Gatti, A. M., Monari, E. & Kirkpatrick, C. J. 2004 Effects of nano-scaled particles on endothelial cell function *in vitro*: studies on viability, proliferation and inflammation. *J. Mater. Sci.* **15**, 321–325. (doi:10.1023/B:JMSM.0000021095.36878.1b)

Revell, P. A., Al-Saffar, N. & Kobayashi, A. 1997 Biological reaction to debris in relation to joint prostheses. *Proc. Inst. Mech. Eng. [H]* **211**, 187–197.

Rodriguez, R. E., Misra, M., Diwan, B. A., Riggs, C. W. & Kasprzak, K. S. 1996 Relative susceptibilities of C57BL/6, (C57BL/6×C3H/He)F_1, and C3H/He mice to acute toxicity and carcinogenicity of nickel subsulfide. *Toxicology* **107**, 131–140. (doi:10.1016/0300-483X(95)03251-A)

Sano, N., Shibata, M., Izumi, K. & Otsuka, H. 1988 Histopathological and immunohistochemical studies on nickel sulfide-induced tumors in F344 rats. *Jpn. J. Cancer Res.* **79**, 212–221.

Schins, R. P. 2002 Mechanisms of genotoxicity of particles and fibers. *Inhal. Toxicol.* **14**, 57–78. (doi:10.1080/089583701753338631)

Shabaan, A. A., Marks, V., Lancaster, M. C. & Dufeu, G. N. 1977 Fibrosarcomas induced by cobalt chloride (CoCl2) in rats. *Lab. Anim.* **11**, 43–46.

Ward, J. J., Thornbury, D. D., Lemons, J. E. & Dunham, W. K. 1990 Metal-induced sarcoma. A case report and literature review. *Clin. Orthop.* **252**, 299–306.